PCCP

Thermodynamic investigations of Sr- and Mg-doped lanthanum gallate by Knudsen effusion mass spectrometry and defect chemical analysis

Aleksandra Matraszek,[a] Lorenz Singheiser,[a] Dietmar Kobertz,[a] Klaus Hilpert,[a] Miroslaw Miller[b] and Manfred Martin[c]

[a] *Research Center Jülich, Institute for Materials and Processes in Energy Systems, 52425, Jülich, Germany*
[b] *Wroclaw University of Technology, Institute of Inorganic Chemistry and Metallurgy of Rare Elements, 50 370, Wroclaw, Poland*
[c] *Aachen University of Technology, Institute of Physical Chemistry, 52056, Aachen, Germany*

Received 10th March 2003, Accepted 13th May 2003
First published as an Advance Article on the web 5th June 2003

The vaporization of the $La_{1-x}Sr_xGa_{1-y}Mg_yO_{3-(x+y)/2}$ perovskite phases was investigated by the use of Knudsen effusion mass spectrometry in the temperature range of 1608–1901 K. The partial pressures of the gaseous species O_2, Mg, Sr, SrO, Ga, GaO, Ga_2O and LaO were determined over the samples investigated. The equilibrium partial pressures were used for the calculation of thermodynamic activities of Ga_2O_3 (1700 K), MgO (1800 K) and SrO (1800 K) in the perovskite phase at the temperatures given in parentheses. The results are compared with the thermodynamic data of $LaGaO_3$(s) without additives. The influence of the Mg concentration on the thermodynamic activity of Ga_2O_3 was carefully studied and modeled by a defect chemical analysis.

Introduction

The $La_{1-x}Sr_xGa_{1-y}Mg_yO_{3-(x+y)/2}$ perovskite phase with different Sr and Mg content has recently been proposed as a possible candidate material for the electrolyte of solid oxide fuel cells (SOFC).[1] First publications on this material were refs. 2 and 3. The material shows good oxygen ion conductivity at about 800 °C,[4] which is comparable to that of ZrO_2 stabilized with 8 mol% Y_2O_3 (YSZ) at 1000 °C. The latter material is commonly used as the solid electrolyte in SOFCs. Electrolytes made of $La_{1-x}Sr_xGa_{1-y}Mg_yO_{3-(x+y)/2}$ are useful for low SOFC operating temperatures. Low operating temperatures between 750 and 800 °C allow serious technological and chemical problems to be avoided. A study of the physicochemical properties of the $La_{1-x}Sr_xGa_{1-y}Mg_yO_{3-(x+y)/2}$ perovskite phase is, therefore, of great practical interest. For example, the incongruent vaporization of material in the different atmospheres at the anode and cathode sides of the SOFC can lead to changes in the chemical composition of the electrolyte and, as a consequence, to a change of its chemical and electrochemical properties. Decomposition of $LaGaO_3$ base perovskites in SOFC by vaporization is reported in refs. 5 and 6 and data on vaporization kinetics by Secondary Ion Mass Spectrometry, SIMS, reported in ref. 7.

In our previous paper[8] we reported first results on the investigation of the equilibrium vaporization of $LaGaO_3$ doped with Sr and Mg by means of Knudsen effusion mass spectrometry. In the present paper we report on the results of systematic equilibrium vaporization studies of the $La_{1-x}Sr_xGa_{1-y}Mg_yO_{3-(x+y)/2}$ perovskite phase. The determination of the thermodynamic activities of the oxide components in the perovskite phase was the aim of these studies. The thermodynamic activities obtained are discussed on the basis of the phase diagram determined by us[9,10] and modeled by a defect chemical analysis.

Experimental

Ten La_2O_3–Ga_2O_3–MgO–SrO samples (denoted A–I in Table 1) of different initial chemical and phase composition were prepared by the sol–gel method, similar to the Pechini method.[10,11] $La(NO_3)_3{\cdot}6H_2O$ (Merck, min. 99.0%), Ga (Chempur, 99.999%), $Mg(NO_3)_2{\cdot}6H_2O$ (Chempur, 99.9+%), $Sr(NO_3)_2$ (Riedel-de-Haean, min. 99%), citric acid and ethylene glycol were used as starting materials in the preparation. Metallic gallium was dissolved in HNO_3 (pure an.) before preparing the sample. The sample was calcined at 1273 K for 20 h in air. The calcined powder was ground in an agate mortar and pressed into pellets. The samples were characterized by XRD after sintering the pellets at 1673 K for 17 h in air. Samples G and H were, in addition, analyzed by the ICP-OES method (instrument 34 000–459 B, Fisons/ARL, Switzerland) to check the deviation from the weighed-in chemical composition of the prepared sample. The relative accuracy of the chemical analysis was ±3%. The results are given in Table 2. Three other samples (J, K, L in Table 1), prepared by the standard solid state reaction method (see ref. 8), were additionally studied in the present work. Details of the samples investigated in the study are given in Table 1.

The vaporization studies of the samples were carried out by Knudsen effusion mass spectrometry at Research Center Jülich (see *e.g.* refs. 12 and 13). The instrument of the MAT 271 type was supplied by Finnigan MAT, Bremen, Germany, and is completely computer-controlled. The vapor species were ionized with an emission current of 1 mA and an electron energy of 70 eV. Knudsen cells made of tungsten and lined completely with iridium were employed in the measurements. Temperatures were measured by an automatic pyrometer of the ETSO-U type supplied by Dr Georg Maurer GmbH, Kohlberg, Germany, and calibrated using the melting points of nickel, silver, gold and platinum.

 DOI: 10.1039/b302696e

Table 1 Initial nominal chemical and phase composition of the La_2O_3–Ga_2O_3–SrO–MgO samples and phase composition of samples after the vaporization study

	Chemical composition					
Sample	$x(\frac{1}{2}La_2O_3)$	x(SrO)	$x(\frac{1}{2}Ga_2O_3)$	x(MgO)	Initial phase composition[a]	Phase composition after KEMS study[a]
A	0.505	–	0.470	0.025	LG, L4G2	LG, L4G2
B	0.505	–	0.445	0.050	LG	LG, L4G2
C	0.505	–	0.420	0.075	LG, L4G2	LG, L4G2
D	0.505	–	0.395	0.100	LG, L4G2	LG, L4G2
E	0.505	–	0.370	0.125	LG, L4G2	LG, L4G2
F	0.505	–	0.345	0.150	LG, L4G2	LG, L4G2
G	0.450	0.050	0.450	0.050	LG, SLG3	LG, SLG, L4G2
H	0.400	0.100	0.400	0.100	LG	LG, SLG, SLG3
I	0.450	0.050	0.400	0.100	LG	LG, x
J	0.500	–	0.375	0.125	LG, L4G2, x	LG, L4G2
K	0.500	–	0.325	0.175	LG, L4G2, x, y	LG, L4G2, x
L	0.425	0.075	0.500	–	LG, SLG3	LG, L4G2, SLG

[a] LG–$LaGaO_3$; L4G2–$La_4Ga_2O_9$; SLG–$SrLaGaO_4$; SLG3–$SrLaGa_3O_7$; x, y–unidentified phases.

Thirty-four runs were performed in order to elucidate the vaporization of the different samples. If the partial pressure of gallium oxide dropped slightly at the beginning of the run, the sample was heated at about 1750 K for 1–5 h until ion intensities became nearly independent of time. This preheating was necessary for initially single-phase samples. The measurement of the ion intensities was subsequently carried out at different decreasing temperatures. Finally, several increasing temperatures were adjusted after reaching the lowest temperature of the measurement range in order to show the reproducibility of the vapor pressure measurements. All runs for the sample in question were performed by evaporating the same material. Between runs, samples were, however, taken off the effusion cell, ground in an agate mortar to refresh the vaporization surface, and then studied again. The phase composition of all samples after the last vaporization run was checked by means of XRD. The residues of samples F (run 24), G (run 28) and H (run 30) were analyzed after the respective run given in parentheses by means of chemical analysis in order to check the change of the sample composition due to the depletion of Ga_2O_3 from the sample during the vaporization study. Results are given in Table 2. Fig. 1 shows as an example the XRD pattern obtained before and after the vaporization study of the sample H.

The calibration of the Knudsen cel–mass spectrometer system was performed by the vaporization of the pure elements and the sample of the phase composition $LaGaO_3$–$La_4Ga_2O_9$ as described in the Results Section.

Results

Ionic species and their assignment to neutral precursors

The ion species O_2^+, Ga^+, Ga_2^+, GaO^+, Ga_2O^+, Mg^+, La^+ and LaO^+ were detected in the mass spectrum of the vapor over all the $La_{1-x}Sr_xGa_{1-y}Mg_yO_{3-(x+y)/2}$ samples. They were identified by their mass, by the shutter effect, and by their isotope abundances. The only exception was run 34 for sample L, where no Mg^+ ion intensity was observed due to the lack of Mg in the sample. Sr^+ and SrO^+ ions were, in addition, detected in samples G, H, I and L, containing strontium. La^+ and LaO^+ were generally only observed at the highest temperatures. The O^+ ion signal originating from the samples was not detected because of interfering background ion intensities at $m/z = 16$ u. The assignment of the Ga-containing ions to their neutral precursors was carried out by the use of isothermal vaporization experiments of the La_2O_3–Ga_2O_3 samples and was reported in ref. 14. It was assumed that the other ion species were formed from the gaseous neutral species as determined by Chupka *et al.*[15] on vaporizing pure La_2O_3 and by Porter *et al.*[16] on vaporizing pure MgO and SrO. Table 3 exemplifies the ion intensities corrected for isotopic distribution, as measured in run 28 at different temperatures on vaporizing the sample G. The ionization/fragmentation scheme is also shown in the Table.

Partial pressures

Partial pressures $p(i)$ of species i at the temperature T were obtained from the equation

$$p(i) = \{kT\Sigma I(i)\}/\sigma(i) \quad (1)$$

where k and $\Sigma I(i)$ are, respectively, the pressure calibration factor and the sum of the intensities of the ions originating from the same neutral precursor i; $\sigma(i)$ is the relative ionization cross section of the species i. The values of the relative ionization cross sections $\sigma(i)$ given in parentheses were used for the following gaseous species i: Ag (5.35), Au (6.82), Ni (5.08), O_2 (1.25), Ga (8.62), GaO (6.12), Ga_2O (18.1), LaO (10.7), Mg (3.39), Sr (8.88) and SrO (6.30). They were estimated as reported in ref. 8.

The pressure calibration was carried out before a series of vaporization studies by vaporizing pure Ag, Au and Ni at their

Table 2 Chemical composition[a] for the La_2O_3–Ga_2O_3–SrO–MgO samples F, G and H before and/or after the vaporization study

	Chemical analysis of initial sample				Chemical analysis after the vaporization study				
Sample	$x(\frac{1}{2}La_2O_3)$	x(SrO)	$x(\frac{1}{2}Ga_2O_3)$	x(MgO)	Run	$x(\frac{1}{2}La_2O_3)$	x(SrO)	$x(\frac{1}{2}Ga_2O_3)$	x(MgO)
F					24	0.547	–	0.309	0.145
G	0.451	0.049	0.451	0.048	28	0.461	0.050	0.439	0.049
H	0.404	0.096	0.402	0.097	30	0.423	0.101	0.374	0.101

[a] Relative uncertainty ±3%.

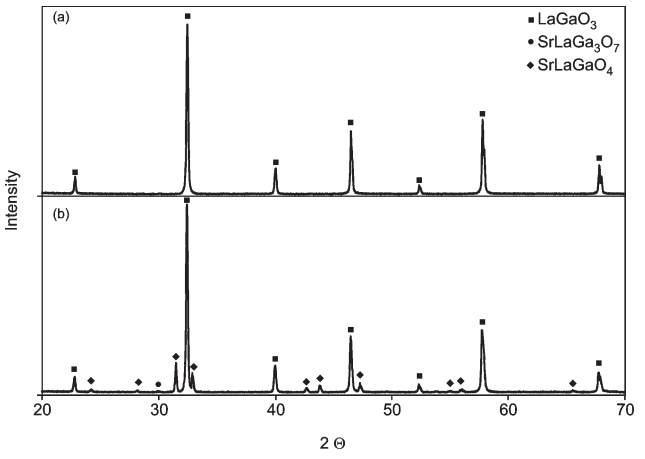

Fig. 1 XRD pattern of sample H before (a) and after the vaporization study (b).

melting temperatures. For this purpose, the ion intensities of the M^+ ions (M = Ag, Au, Ni) were measured at the well established melting point of the respective metal and the value of k was calculated independently from eqn. (1) for the three calibration substances. The mean of the three k values determined in this way was used to calculate the partial pressures upon vaporizing the $La_{1-x}Sr_xGa_{1-y}Mg_yO_{3-(x+y)/2}$ samples. Stability of the calibration factor in the course of the investigations was checked by repeating the calibration procedure for pure Ni. The respective correction was then used to obtain the current k value. The stability of the calibration factor amounted to ±12% during the study for over one year. The main reason for the nearly constant sensitivity of our mass spectrometer was the continuous operation of the ion source, which was not switched off between runs. Moreover, the positioning of the effusion orifice was reproducible due to the mechanical and optical arrangement. The same cover of the Knudsen cell was used in the vaporization experiments of samples and calibration substances to guarantee identical dimensions and geometry of the effusion orifice. To avoid vapor condensation inside of the Knudsen cell cover, its temperature was kept somewhat higher in comparison to the sample surface (about 20 K at 1700 K).

Partial pressures were evaluated by the use of eqn. (1) for each measuring temperature. In Fig. 2 we show as an example the partial pressures of vapor species obtained in run 28 for sample G. Tables 4 and 5 contain the partial pressure equations of the different species obtained for all runs.

Thermodynamic activities

The determination of the thermodynamic activities of MgO and SrO in the samples was carried out by vaporizing pure MgO and SrO before and after the measurement of a sample. the equilibria

$$MgO = \mathrm{Mg(g)} + 1/2\ \mathrm{O_2(g)}, \quad (2)$$

$$SrO = \mathrm{SrO(g)}, \quad (3)$$

were evaluated from the measurements of the sample materials and the pure components. MgO and SrO denote the respective oxide components dissolved in the $La_{1-x}Sr_xGa_{1-y}Mg_y$-$O_{3-(x+y)/2}$ samples or these oxides as pure materials.

The thermodynamic activity of Ga_2O_3 in the samples was determined by comparing their mass spectra with the mass spectrum of the Ga_2O_3–La_2O_3 sample, $x(Ga_2O_3) = 0.40$, consisting of the two phases $LaGaO_3$(s) and $La_4Ga_2O_9$(s). The thermodynamic activity of Ga_2O_3 in this sample at 1700 K was previously determined by us using mass spectrometry.[14] Direct comparison of ion intensities detected for the latter sample with those recorded for the $La_{1-x}Sr_xGa_{1-y}Mg_y$-$O_{3-(x+y)/2}$ sample enables the most accurate study of the influence of the second group element concentration in the perovskite phase on the activity of gallium oxide at 1700 K. The mass spectrum of the $\{LaGaO_3(s) + La_4Ga_2O_9(s)\}$ sample was measured for this purpose before and after studying the vaporization of each sample. The equilibrium

$$Ga_2O_3 = \mathrm{Ga_2O(g)} + \mathrm{O_2(g)} \quad (4)$$

was considered in the measurements of the sample materials and the reference $\{LaGaO_3(s) + La_4Ga_2O_9(s)\}$ sample. The variation of the ion intensities measured for the reference sample and used in this evaluation at 1700 K in the experiment series performed for over four months was lower than 10 per cent in case of O_2^+ and lower than 14 per cent in case of Ga_2O^+.

The following equations finally result for the computation of the thermodynamic activities by considering the equilibrium constants $K^\circ_p(2)$, $K^\circ_p(3)$ and $K^\circ_p(4)$ of the reactions (2)–(4) and eqn. [1]:

$$a(\mathrm{MgO}) = \frac{I(\mathrm{Mg^+})I(\mathrm{O_2^+})^{1/2}}{I^0(\mathrm{Mg^+})I^0(\mathrm{O_2^+})^{1/2}}, \quad (5)$$

$$a(\mathrm{SrO}) = \frac{I(\mathrm{SrO^+})}{I^0(\mathrm{SrO^+})}, \text{ and} \quad (6)$$

$$a(\mathrm{Ga_2O_3}) = \frac{I(\mathrm{Ga_2O^+})I(\mathrm{O_2^+})}{I^0(\mathrm{Ga_2O^+})I^0(\mathrm{O_2^+})}. \quad (7)$$

Table 3 Ion intensities (in s^{-1}) at different temperatures corrected for isotopic distribution obtained for sample G in run 28 and assignment of the ions to neutral molecules

	T/K	O_2(g) → O_2^+	Ga(g) → Ga^+	Ga_2O(g) → Ga_2O^+	→ Ga_2^+	GaO(g) → GaO^+	LaO(g) → La^+	→ LaO^+	Mg(g) → Mg^+	Sr(g) → Sr^+	SrO(g) → SrO^+
1	1828	6.44×10^3	8.55×10^4	1.78×10^4	2.92×10^3	6.23×10^2	9.4	1.45×10^1	2.60×10^2	4.10×10^1	1.01×10^1
2	1787	2.92×10^3	3.79×10^4	6.65×10^3	1.04×10^3	2.47×10^2	4.9	5.9		2.43×10^1	4.5
3	1767	1.76×10^3	2.54×10^4	4.10×10^3	6.81×10^2	1.53×10^2	3.2	5.0		1.78×10^1	5.4
4	1734	1.17×10^3	1.58×10^4	2.27×10^3	3.60×10^2	9.36×10^1				9.5	3.5
5	1708	8.81×10^2	9.88×10^3	1.30×10^3	1.98×10^2	7.12×10^1		1.7		7.8	3.4
6	1682	5.74×10^2	6.11×10^3	8.19×10^2	1.39×10^2	3.69×10^1				6.4	
7	1661	3.40×10^2	3.85×10^3	5.40×10^2	9.27×10^1	2.44×10^1					
8	1793	3.30×10^3	4.21×10^4	6.88×10^3	1.12×10^3	2.74×10^2	3.2	9.2		2.07×10^1	5.9
9	1825	6.24×10^3	8.31×10^4	1.56×10^4	2.55×10^3	6.23×10^2	7.8	1.27×10^1	2.46×10^2	2.76×10^1	8.9
10	1853	1.02×10^4	1.31×10^5	2.84×10^4	4.38×10^3	9.56×10^2	9.2	2.30×10^1	3.81×10^2	3.38×10^1	9.6
11	1755	1.61×10^3	2.14×10^4	3.22×10^3	5.29×10^2	1.34×10^2	1.7	4.9		1.39×10^1	3.0
12	1809	4.50×10^3	5.75×10^4	1.01×10^4	1.60×10^3	3.58×10^2	3.4	7.6	2.24×10^2	1.97×10^1	7.8

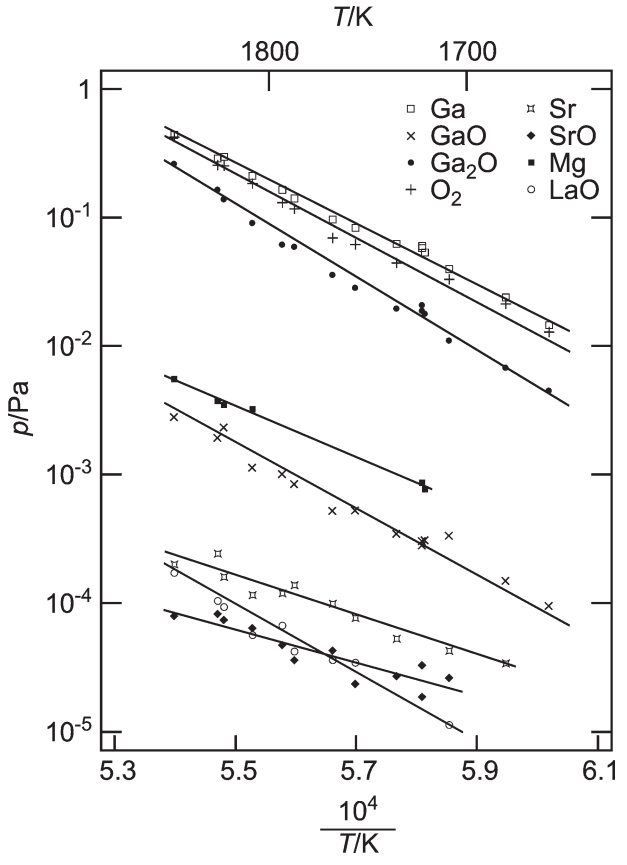

Fig. 2 Partial pressures over sample G (*cf.* Table 1) at different temperatures (run 28).

$I^{\circ}(i)$ denotes the ion intensities detected on vaporizing the respective reference material. Thermodynamic activities were obtained by interpolation for temperatures of 1700 K (Ga_2O_3) and of 1800 K (MgO, SrO) for each of the runs 1–34 by using eqns. (5)–(7).

The activity of La_2O_3 at 1800 K could only be estimated due to the very small intensities of the ions La^+ and LaO^+ observed on vaporizing the $La_{1-x}Sr_xGa_{1-y}Mg_yO_{3-(x+y)/2}$ samples. The estimation was performed by considering the equilibrium:

$$La_2O_3(s) = 2\ LaO(g) + \tfrac{1}{2}\ O_2(g) \qquad (8)$$

for the sample material and for the reference sample $\{LaGaO_3(s) + La_4Ga_2O_9(s)\}$. The thermodynamic activity of La_2O_3 in the latter sample at 1800 K was previously determined by us as $a(La_2O_3) = 0.47$.[14] The thermodynamic activity of lanthanum oxide in the $La_{1-x}Sr_xGa_{1-y}Mg_yO_{3-(x+y)/2}$ sample was evaluated from the equation

$$a(La_2O_3) = \frac{\left\{I(LaO^+)^2 I(O_2^+)^{1/2}\right\}_{LSGM}}{\left\{I(LaO^+)^2 I(O_2^+)^{1/2}\right\}_{LG}} 0.47 \qquad (9)$$

where LSGM and LG indicate that the ion intensities were measured over the sample $La_{1-x}Sr_xGa_{1-y}Mg_yO_{3-(x+y)/2}$ and the sample $\{LaGaO_3(s) + La_4Ga_2O_9(s)\}$, respectively.

Table 6 summarizes the thermodynamic activities of the components in the $La_{1-x}Sr_xGa_{1-y}Mg_yO_{3-(x+y)/2}$ samples obtained in all runs. The thermodynamic activity of Ga_2O_3 was evaluated for a temperature of 1700 K by taking also into account the temperature range used in ref. 14 for the vaporization study of the reference sample $\{LaGaO_3(s) + La_4Ga_2O_9(s)\}$. The thermodynamic activities of MgO(s) and SrO(s) were evaluated at the comparatively high temperature of 1800 K due to the lower volatility of these components in comparison to gallium oxide. For comparison, the thermodynamic activities of Ga_2O_3 were recalculated for 1800 K by assuming that the chemical potential of Ga_2O_3 in the $La_{1-x}Sr_xGa_{1-y}Mg_yO_{3-(x+y)/2}$ samples is independent of temperature. This assumption is based on the general experience that the Gibbs energy of formation of the perovskites from their component oxides is practically temperature-independent. The values of $a(Ga_2O_3)$ obtained in this way at 1800 K are also reported in Table 6.

Discussion

Partial pressures and condensed phase equilibria

Partial pressures and thermodynamic activities of the components depend on the phase composition of the sample being in equilibrium with the vapor. Phase equilibria in the La_2O_3–Ga_2O_3–SrO and La_2O_3–Ga_2O_3–MgO subsystems were studied by Majewski *et al.*[17,18] and by us.[9] The quasi-ternary system $LaGaO_3$–"$LaSrO_{2.5}$"–"$LaMgO_{2.5}$" was, in addition, studied by three groups.[10,18,19] Data obtained in the present study generally confirm the phase relations reported in the cited studies.

According to different studies, the solubility of Mg in the $LaGaO_3$ perovskite phase at 1400 °C amounts to at least 20 mol% of the Ga sites. In contrast to this, the solubility of Sr in the $LaGaO_3$ perovskite phase is significantly lower, ranging from 3 mol%[9,10] up to 8 mol%[17] of the La sites depending on different studies. Therefore, only one ternary La_2O_3–Ga_2O_3–SrO sample (sample L in Table 1) was investigated in the present study. This sample consists of the three phases (La,Sr)GaO_3, $SrLaGaO_4$ and $SrLaGa_3O_7$ according to the phase diagram of the La_2O_3–Ga_2O_3–SrO system.[9] XRD analysis of the sample before the vaporization study shows the pattern from only two of these phases. The $SrLaGaO_4$ phase could not be identified, probably because of a too small amount of the phase in the sample.

A vaporization study of $La_{1-x}Sr_xGaO_{3-x/2}$, $x = 0.5$, 0.10, 0.20, 0.25, 0.30 and 0.35, showed that the partial pressures of Ga_2O_3 over these samples agree with each other within the experimental reproducibility.[20] This confirms that all these samples consist of three phases. The $LaGaO_3$ perovskite phase is one of these equilibrium phases. It contains the maximal fraction of Sr (probably less than 5 mol% Sr on the La sites).

The initial chemical compositions of the ternary La_2O_3–Ga_2O_3–MgO samples A–F were chosen in such a way that $\{x(\frac{1}{2}Ga_2O_3) + x(MgO)\}/x(\frac{1}{2}La_2O_3) = 0.98$. This composition would correspond to a 2 mol% B-deficient perovskite, $La(Ga_{1-y}Mg_y)_{0.98}O_{3-\delta}$. Due to the narrow homogeneity range of the perovskite phase concerning different La/Ga ratios, the samples correspond to the two-phase field $\{La(Ga,Mg)O_3(s) + La_4(Ga,Mg)_2O_9(s)\}$, the perovskite phase being the main one. This was generally confirmed by the XRD pattern of the initial samples (Table 1). Considering the La_2O_3–Ga_2O_3–MgO phase diagram and tie lines between the two phases La(Ga,Mg)O_3(s) and $La_4(Ga,Mg)_2O_9$(s), it can be assumed that the chemical composition of perovskite in equilibrium in the samples is $LaGa_{1-y}Mg_yO_{3-y/2}$. XRD analysis of the residue of samples A–F showed in all cases bigger intensities of the $La_4Ga_2O_9$(s) phase pattern in comparison to the initial sample due to partial depletion of Ga_2O_3 during the vaporization study. This depletion was also confirmed by chemical analysis of the residue of sample F (Table 1). The Ga_2O_3 depletion does not greatly change the composition of the equilibrium perovskite phase, as follows from the phase diagram.

Ion intensities and – therefore – also the vapor pressures recorded in runs 1–24 involving samples A–F were nearly time-independent from the beginning of the vaporization experiments. This was not the case for the vaporization study of samples J and K. Partial pressures of gallium-containing

Table 4 Parameters of the partial pressure equation $\ln p(i)/\mathrm{Pa} = A/T + B$ obtained for the main gaseous species over different ternary La_2O_3–Ga_2O_3–MgO samples

				p(Mg)/Pa		$p(O_2)$/Pa		p(Ga)/Pa		$p(Ga_2O)$/Pa	
Sample	Run	ΔT/K	n^a	A	B	A	B	A	B	A	B
A	1	1608–1790	16	−70 802	30.232	−59 907	31.719	−59 589	32.008	−68 252	35.819
				±2229	±1.275	±2247	±1.329	±2466	±1.459	±1678	±0.993
A	2	1624–1843	15	−52 206	22.810	−59 437	31.436	−55 575	29.509	−66 261	34.646
				±619	±0.344	±1566	±0.903	±1274	±0.736	±1339	±0.774
A	3	1647–1880	12	−64 480	29.899	−57 826	30.552	−52 829	27.930	−66 057	34.475
				±1495	±0.812	±1142	±0.647	±1157	±0.657	±1118	±0.635
B	4	1653–1841	15	−65 528	30.464	−62 378	32.782	−56 503	29.742	−65 606	33.847
				±7227	±4.039	±1915	±1.094	±696	±0.399	±1323	±0.759
B	5	1671–1861	11	−55 904	25.282	−62 323	32.737	−55 467	29.063	−65 650	33.857
				±1713	±0.952	±1294	±0.730	±1047	±0.594	±1905	±1.081
B	6	1689–1850	10	−51 171	22.811	−58 787	30.846	−50 922	26.529	−66 577	34.385
				±1466	±0.817	±3996	±2.261	±1644	±0.932	±1835	±1.040
B	7	1662–1841	11	−51 038	22.953	−61 344	32.180	−55 540	29.254	−65 788	33.887
				±1767	±0.983	±3121	±1.781	±1177	±0.672	±1516	±0.865
B	8	1675–1837	11	−49 013	21.986	−61 176	32.033	−56 996	29.988	−66 103	33.989
				±2405	±1.348	±2561	±1.456	±1088	±0.621	±1491	±0.851
C	9	1701–1888	11	−49 749	22.463	−57 044	29.793	−58 550	30.567	−69 950	35.911
				±1591	±0.869	±1532	±0.853	±818	±0.455	±1250	±0.695
C	10	1715–1900	13	−47 200	21.170	−59 957	31.355	−53 502	27.674	−67 973	34.823
				±1547	±0.845	±1180	±0.652	±703	±0.388	±1702	±0.941
D	11	1652–1872	15	−51 226	23.567	−61 107	31.636	−58 844	30.718	−65 445	33.192
				±3774	±2.122	±3428	±1.945	±1334	±0.763	±1942	±1.111
D	12	1650–1830	15	−57 619	27.101	−55 957	28.581	−60 228	31.455	−62 180	31.235
				±2967	±1.665	±3389	±1.926	±1530	±0.877	±2252	±1.290
D	13	1671–1840	9	−54 007	25.107	−51 624	26.220	−56 776	29.461	−63 146	31.774
				±1572	±0.882	±2713	±1.542	±2040	±1.159	±2362	±1.342
D	14	1646–1835	15	−58 912	27.843	−50 336	25.445	−54 899	28.383	−61 517	30.840
				±2094	±1.178	±2549	±1.462	±1054	±0.607	±1378	±0.793
E	15	1680–1846	13	−55 490	25.913	−49 245	25.277	−54 640	28.248	−62 052	31.152
				±1981	±1.117	±1461	±0.830	±1284	±0.729	±1691	±0.960
E	16	1683–1879	13	−54 429	25.377	−47 784	24.595	−51 127	26.337	−65 190	33.160
				±2372	±1.308	±2274	±1.276	±1058	±0.594	±1718	±0.964
E	17	1729–1901	9	−50 525	23.166	−57 544	29.754	−51 155	26.149	−68 674	34.792
				±840	±0.456	±854	±0.467	±995	±0.548	±1125	±0.615
F	18	1623–1834	13	−59 275	28.232	−47 341	24.076	−54 976	28.584	−59 933	30.251
				±609	±0.339	±1630	±0.940	±1149	±0.666	±1207	±0.700
F	19	1650–1848	12	−56 515	26.689	−51 259	26.242	−52 735	27.229	−59 260	29.904
				±2206	±1.228	±1658	±0.948	±815	±0.466	±1212	±0.692
F	20	1667–1821	10	−63 045	30.273	−46 379	23.404	−51 398	26.453	−56 208	28.058
				±3882	±2.172	±2525	±1.439	±1227	±0.703	±1835	±1.051
F	21	1652–1850	12	−52 921	24.649	−49 726	25.238	−52 283	26.913	−57 321	28.662
				±1844	±1.024	±1354	±0.772	±605	±0.345	±1310	±0.747
F	22	1668–1796	11	−50 786	23.357	−48 262	24.398	−50 566	25.933	−55 637	27.659
				±3458	±1.972	±2199	±1.261	±716	±0.415	±2021	±1.167
F	23	1630–1840	13	−51 658	23.952	−54 119	27.769	−53 221	27.481	−60 512	30.480
				±2769	±1.570	±1810	±1.030	±1080	±0.624	±1253	±0.724
F	24	1628–1827	14	−51 172	23.724	−46 526	23.495	−52 346	27.078	−58 701	29.515
				±1529	±0.868	±1662	±0.965	±1605	±0.932	±1590	±0.923
J	25	1638–1922	14	−61 083	31.276	−50 672	23.262	−55 577	28.847	−65 647	33.503
				±1489	±0.823	±821	±0.463	±796	±0.449	±1192	±0.672
K	26	1649–1882	13	−55 640	25.810	−56 534	28.724	−57 217	29.417	−65 236	33.049
				±898	±0.510	±3484	±1.920	±827	±0.470	±1042	±0.592

[a] Number of measurements within a run.

species dropped slightly at the beginning of runs 25 and 26 involving these ternary samples and became nearly constant after 1–5 h of vaporization at about 1750 K. These runs started at a comparatively high measurement temperature only after the ion intensities became time-independent.

The different behavior in the initial stage of vaporization observed for samples A–F in comparison to samples J and K can be explained as follows. The initial chemical compositions of samples J and K correspond to the pure perovskite phase (Table 1). Due to the depletion of Ga_2O_3, the thermodynamic activity of Ga_2O_3 changed within the homogeneity range of this phase as follows from the phase diagram. Once a second phase had become stable in the Knudsen cell, the partial pressures and thus also a depletion of gallium oxide became substantially lower leading to the practically time-independent ion intensities in the mass spectrum. An XRD pattern of the $La_4Ga_2O_9$(s) phase with low intensities was identified after the vaporization of the two samples J and K in addition to the pattern of the main Ga_2O_3-poor perovskite phase as follows from Table 1.

Table 5 Parameters of the partial pressure equations $\ln p(i)/\mathrm{Pa} = A/T + B$ obtained for the main gaseous species over the different La_2O_3–Ga_2O_3–SrO–MgO samples, G, H, I and over the $La_{0.85}Sr_{0.15}GaO_{2.925}$ sample, L

				$p(Mg)$/Pa		$p(O_2)$/Pa		$p(Ga)$/Pa		$p(Ga_2O)$/Pa		$p(Sr)$/Pa		$p(SrO)$/Pa	
Sample	Run	ΔT/K	n^a	A	B	A	B	A	B	A	B	A	B	A	B
G	27	1666–1820	13	−52 653	23.338	−60 616	31.858	−52 924	27.794	−66 000	34.150	−37 920	12.138	−43 067	13.898
				±2229	±1.245	±2415	±1.363	±1114	±0.634	±1891	±1.076	±2341	±1.332	±7947	±4.450
G	28	1661–1853	12	−45 287	19.275	−54 440	28.391	−51 851	27.137	−63 514	32.799	−35 654	10.858	−30 499	7.087
				±1188	±0.668	±1855	±1.051	±1409	±0.803	±2025	±1.154	±3119	±1.758	±4321	±2.437
H	29	1642–1838	14	−77 345	37.595	−44 564	22.940	−52 151	27.340	−60 944	31.330	−36 337	11.294	−46 647	15.794
				±7821	±4.340	±1558	±0.891	±1477	±0.843	±2111	±1.204	±2053	±1.171	±2411	±1.357
H	30	1650–1872	14	−63 359	29.879	−48 143	25.024	−51 333	26.925	−60 748	31.214	−37 748	11.943	−48 566	16.905
				±5520	±3.053	±1159	±0.656	±1164	±0.659	±1815	±1.027	±1765	±0.994	±2237	±1.262
I	31	1650–1835	12	−54 779	25.072	−60 519	31.532	−57 388	30.151	−63 479	32.334	−32 794	8.889	−55 435	20.337
				±2436	±1.369	±1901	±1.085	±1314	±0.750	±1679	±0.958	±3520	±2.009	±3388	±1.893
I	32	1659–1848	12	−55 385	25.379	−60 407	31.407	−59 851	31.544	−64 355	32.771	−25 121	4.566	−59 467	22.242
				±2378	±1.332	±2260	±1.281	±968	±0.548	±1540	±0.873	±3237	±1.834	±8055	±4.496
I	33	1665–1852	12	−66 747	31.605	−60 437	31.327	−57 759	30.267	−63 760	32.344	−27 564	6.011	−47 862	15.999
				±2586	±1.427	±2082	±1.178	±1272	±0.720	±1739	±0.984	±4654	±2.634	±3233	±1.804
L	34	1632–1888	15	–	–	−66 381	34.832	−57 770	30.266	−67 512	35.249	−40 835	14.355	−49 814	18.300
						±2220	±1.243	±1113	±0.634	±1357	±0.773	±1327	±0.756	±2917	±1.653

[a] Number of measurements within a run.

The $La_{1-x}Sr_xGa_{1-y}Mg_yO_{3-(x+y)/2}$ quasi-quaternary samples G, H, I vaporize in a manner similar to the quasi-ternary samples. Ion intensities of Ga-containing species were not stable in first runs with fresh material for about 2 h. The chemical analysis of residues of these samples (see Table 1) also confirms a depletion of gallium oxide from these samples. The XRD pattern of the residues (Table 1 and Fig. 1) shows mainly formation of the gallium-poor phases $SrLaGaO_4$(s) and $La_4(Ga,Mg)_2O_9$(s) by the vaporization. Formation of these phases can be explained by the quasi-quaternary phase diagram.[9,18]

Before the vaporization study, the sample G contained traces of the $SrLaGa_3O_7$(s) phase in addition to the main perovskite phase as follows from the XRD pattern. This can be explained by incomplete reactions during the sample preparation.

Thermodynamic activities

Results obtained for the ternary $LaGa_{1-y}Mg_yO_{3-y/2}$ samples J and K prepared by the standard solid-state reaction method agree reasonably well with the data obtained for the samples A–F prepared by a sol–gel method. This confirms the thermodynamic equilibrium in the Knudsen cell in the present study.

The thermodynamic activity of Ga_2O_3 in the sample L agrees within the error limits with a value of 2.17×10^{-3}, obtained for the pure gallium-poor $LaGaO_3$(s) phase.[14] This can be explained by the observed low solubility of Sr in this phase. Moreover, the substitution of La atoms by Sr is not expected to greatly influence the thermodynamics of the Ga sublattice in the perovskite phase. The thermodynamic activity of SrO in the sample was nearly 1 in spite of the fact that the pure SrO(s) phase was not detected in the sample. Ion intensities of Sr^+ and SrO^+ were larger than those from pure SrO(s) and time-dependent at the beginning of the run. We believe that this phenomenon is due to the contamination of the sample with a small amount of $Sr(OH)_2$ giving rise to the formation of Sr^+ and SrO^+ ions as fragments. The value of a(SrO) obtained in the present study for sample L is, therefore, not recommended and given in parentheses (see Table 6).

A substitution of Ga atoms by Mg in the perovskite phase lowers, as expected, the thermodynamic activity of Ga_2O_3. Fig. 3 shows the dependence of $a(Ga_2O_3)$ in the Ga_2O_3-poor perovskite phase at 1700 K as a function of the Mg mole fraction in this phase. Mean values of activities and their standard deviations obtained for each composition in different runs are presented in the graph.

The thermodynamic activity of MgO in the perovskite phase $LaGa_{1-y}Mg_yO_{3-y/2}$ ranges from 0.41 for $y = 0.05$ up to 1 for $y = 0.25$. This means strong positive deviations from ideality for this component and agrees with the phase diagram of the ternary system. Pure MgO(s) is the third phase which is formed in this system in addition to $La(Ga,Mg)O_{3-\delta}$(s) and $La_4(Ga,Mg)_2O_{9-\delta}$ outside the solubility range of Mg in the perovskite phase. Similar positive deviations from ideality were previously identified by us on studying the thermochemistry of the $LaCrO_3$ perovskite phase doped with Mg atoms.[21]

As can be seen in Table 6, for some samples the activity values of components show a slight trend for a sequence of vaporization experiments using the same material. Sample B exemplifies, for instance, this phenomenon for the activities of Ga_2O_3 and MgO and sample F for the activity of Ga_2O_3. These quasi-ternary samples consisted of two phases after the vaporization study, as follows from Table 1. In this case the system is not thermodynamically invariant and the thermodynamic activities of components are expected to still depend on the chemical composition of the sample. As already mentioned, the chemical composition changed during the incongruent vaporization of samples towards the Ga-poor phases. This was confirmed by the chemical analysis performed for residues of samples F, G and H after the vaporization study. The change of the chemical composition of the quasi-ternary sample La_2O_3–Ga_2O_3–MgO composed initially of perovskite phase and a small amount of $La_4(Ga,Mg)_2O_{9-\delta}$ phase is schematically shown in Fig. 4. It was assumed according to experimental observation and chemical analysis of the residue of sample F that Ga_2O_3 and also MgO depleted from the material. The line schematically represents a continuous change of composition during the vaporization experiments. This line crosses the tie-lines of the two-phase field in a way which results in increasing the MgO and decreasing the Ga_2O_3 mole fraction in the perovskite equilibrium phase. The latter leads to the respective changes of the thermodynamic activities of these components.

A comment should be finally made on the thermodynamic activities obtained in the present study for the quasi-quaternary samples G, H and I. The thermodynamic activities of MgO in these samples show similar positive deviations from ideality as in the quasi-ternary samples A–F. The SrO activity was determined for these samples with good reproducibility in contrast to the quasi-ternary sample L. This can be explained

Table 6 Thermodynamic activities of Ga_2O_3 at 1700 and 1800 K and those of other components at 1800 K obtained in all the runs on vaporizing the different La_2O_3–Ga_2O_3–SrO–MgO samples

Sample	Run	$a(Ga_2O_3) \times 10^3$ (1700 K)	$a(Ga_2O_3) \times 10^3$ (1800 K)[a]	a(MgO)	$a(La_2O_3)$[b]	a(SrO)
LG-L4G2[c]	Ref. 14	2.17	3.35	–	0.47	–
A	1	1.83	2.60	–	–	–
A	2	1.78	2.53	0.35	0.31	–
A	3	1.83	2.60	0.47	0.20	–
Mean value		*1.81 ± 0.03*	*2.58 ± 0.04*	*0.41 ± 0.08*	*0.26 ± 0.08*	
B	4	1.39	2.00	0.38	0.98	–
B	5	1.22	1.77	0.46	0.33	–
B	6	1.59	2.27	0.56	0.45	–
B	7	1.26	1.83	0.64	0.44	–
B	8	1.09	1.59	0.75	0.28	–
Mean value		*1.31 ± 0.19*	*1.89 ± 0.26*	*0.56 ± 0.15*	*0.50 ± 0.28*	
C	9	1.18	1.72	0.84	–	–
C	10	1.09	1.59	0.92	0.18	–
Mean value		*1.14 ± 0.06*	*1.66 ± 0.09*	*0.88 ± 0.06*	*0.18*	
D	11	1.05	1.54	0.90	0.20	–
D	12	1.07	1.56	0.81	0.17	–
D	13	1.06	1.55	0.83	0.15	–
D	14	1.02	1.50	0.83	0.26	–
Mean value		*1.05 ± 0.02*	*1.54 ± 0.03*	*0.84 ± 0.04*	*0.20 ± 0.05*	
E	15	1.13	1.65	1.01	0.28	–
E	16	1.59	2.27	1.15	0.57	–
E	17	0.798	1.19	0.99	0.08	–
Mean value		*1.17 ± 0.40*	*1.70 ± 0.54*	*1.05 ± 0.09*	*0.43 ± 0.21*	
F	18	1.06	1.55	1.15	0.51	
F	19	0.942	1.39	1.11	0.22	–
F	20	0.932	1.37	1.02	0.17	–
F	21	0.769	1.15	0.98	0.24	–
F	22	0.722	1.08	0.89	–	–
F	23	0.655	0.98	1.04	0.18	–
F	24	0.698	1.05	1.06	0.29	–
Mean value		*0.83 ± 0.15*	*1.22 ± 0.21*	*1.04 ± 0.09*	*0.27 ± 0.13*	
J	25	0.630	0.95	1.05	0.68	–
K	26	0.697	1.04	0.833	0.19	–
G	27	2.04	2.88	0.42	> 1	0.37
G	28	2.64	3.67	0.41	> 1	0.44
Mean value		*2.34 ± 0.42*	*3.28 ± 0.56*	*0.42 ± 0.01*		*0.41 ± 0.05*
H	29	4.26	5.77	0.69	0.20	0.34
H	30	4.15	5.63	0.77	0.20	0.36
Mean value		*4.21 ± 0.08*	*5.70 ± 0.10*	*0.73 ± 0.06*	*0.20 ± 0.00*	*0.35 ± 0.01*
I	31	1.18	1.72	0.63	0.10	0.24
I	32	1.03	1.51	0.58	0.22	0.17
I	33	0.863	1.28	0.53	0.09	0.21
Mean value		*1.02 ± 0.16*	*1.50 ± 0.22*	*0.58 ± 0.05*	*0.14 ± 0.07*	*0.21 ± 0.04*
L	34	2.01	2.84	–	0.14	(0.74)[d]
M[e]	Ref. 8	3.38	4.64	0.61	0.38	0.36
M[e]	Ref. 8	2.70	3.75	0.64	0.37	0.28
Mean value		*3.04 ± 0.48*	*4.20 ± 0.63*	*0.63 ± 0.02*	*0.38 ± 0.01*	*0.32 ± 0.06*

[a] Calculated from the value at 1700 K assuming the chemical potential of Ga_2O_3 at 1700 K and at 1800 K to be the same. [b] Estimated from eqn. (9). [c] Two-phase sample $\{LaGaO_3(s) + La_4Ga_2O_9(s)\}$. [d] Not recommended due to the probable existence of non-equilibrium phases in the sample. [e] Sample composition is $La_{0.85}Sr_{0.15}Ga_{0.85}Mg_{0.15}O_{2.85}$, see also the Discussion Section.

by the different preparation method in the case of the quasi-quaternary samples which can avoid the formation of non-equilibrium Sr containing phases. SrO shows positive deviations from ideality by analogy to MgO.

The thermodynamic activity of Ga_2O_3 in the samples G and H is similar to those in the pure $LaGaO_3$ phase in spite of a lower Ga_2O_3 concentration in these samples. This seems to be in contradiction to the thermodynamic rules. An explanation

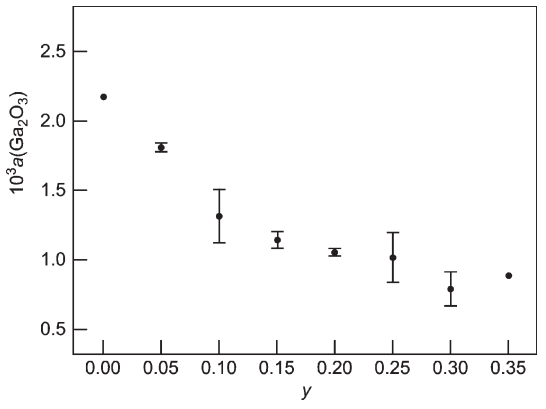

Fig. 3 Thermodynamic activities of Ga_2O_3 in samples of the composition $LaGa_{1-y}Mg_yO_{3-y/2}$ at 1700 K as a function of the Mg content, y.

for this phenomenon could be the defect formation in the perovskite phase due to the substitution of a trivalent atom by a divalent one. This substitution is expected to increase the Gibbs energy of formation of the phase and thus also the thermodynamic activities of the components.[22,23] However, we do not observe a similar effect in the case of the quasi-ternary samples A–F. Another explanation for this observation may be the effect of a change of chemical composition of phases (including the Ga-poor perovskite phase) on temperature. The thermodynamic activities of Ga_2O_3 and SrO in sample I are substantially lower in comparison to other quasi-quaternary samples. This is probably because of the different phase composition of the sample after partial depletion of Ga_2O_3 in the course of the vaporization study. It should be mentioned that this depletion can result in the formation of small amounts of other phases in addition to those which are identified by means of XRD analysis. Therefore, the phase composition given in Table 1 for samples G, H and I should not be considered as complete.

The sample M (see Table 6) of the chemical composition $La_{0.85}Sr_{0.15}Ga_{0.85}Mg_{0.15}O_{2.85}$ has been investigated previously by us and the results obtained are reported in ref. 8 (see sample B in ref. 8). The measurement in ref. 8 was reevaluated by using the $\{LaGaO_3(s) + La_4Ga_2O_9(s)\}$ sample as reference material in contrast to ref. 8 where pure $Ga_2O_3(s)$ was used as reference material. The reevaluated value at 1700 K, $a(Ga_2O_3) = 3.04 \times 10^{-3}$, is given in Table 6 together with the values for a(SrO) and a(MgO) from ref. 8.

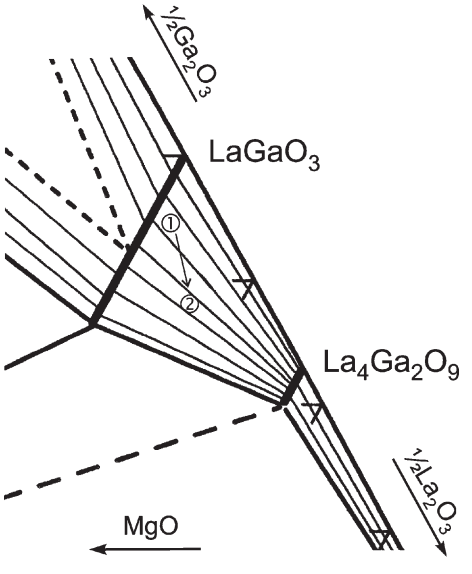

Fig. 4 Schematic representation of the chemical composition change of a quasi-ternary MgO–Ga_2O_3–La_2O_3 sample due to incongruent vaporization; 1- initial composition, 2-composition after the vaporization study.

The sample I studied in the present work is nominally of the same composition $La_{0.90}Sr_{0.10}Ga_{0.80}Mg_{0.20}O_{2.85}$ as sample C studied in ref. 8. The sample material studied in ref. 8 was supplied by ECN, Petten, The Netherlands, whereas the material studied in the present work was prepared by ourselves (see Experimental Section). The values reported in ref. 8 ($a(Ga_2O_3) = 1.7 \times 10^{-3}$, a(MgO) = 0.70, a(SrO) = 0.30) for a temperature of 1800 K agree reasonably well with those of this work (*cf.* Table 6). The small difference of the values might be caused by different phase composition of the sample after the vaporization study in ref. 8 in comparison to the present work. Unfortunately, the residue of sample C in ref. 8 was not studied by means of XRD.

Uncertainties of data

Probable overall uncertainties were not evaluated for the partial pressures given in Tables 4 and 5 since it is difficult to estimate uncertainties for the ionization cross sections of gaseous oxide species. In contrast to the partial pressures, the thermodynamic activities do not depend on ionization cross sections but only on ion intensity ratios. This leads to comparatively small uncertainties for the thermodynamic activities. These uncertainties were estimated as ±30%, ±30% and ±20% for the activities of Ga_2O_3, MgO and SrO, respectively, considering the reproducibility of measurements. The absolute error of the temperature measurement estimated as ±10 K was additionally used in the error estimation for the thermodynamic activities. The thermodynamic activities of La_2O_3 in samples should be regarded as estimated.

Defect chemical modeling of the chemical activities in $La(Ga_{1-y}Mg_y)O_{3-y/2}$

In this section the observed dependence of the measured chemical activities of Ga_2O_3 and MgO on the dopand fraction, y, will be modeled using a defect chemical analysis. The analysis will only be performed for Mg-doped lanthanum gallate, $LaGa_{1-y}Mg_yO_{3-y/2}$ (LGM), where the activities of Ga_2O_3 and MgO as well have been measured as a function of the Mg-fraction, y (see Table 6 and Fig. 3).

$LaGa_{1-y}Mg_yO_{3-y/2}$ is a quaternary system which has five thermodynamic degrees of freedom within its stability field. These independent thermodynamic variables are the total pressure, p, the temperature, T, the Mg-fraction, y, the oxygen activity, a_{O_2}, and the activity of one oxide component, *e.g.* $a_{La_2O_3}$. To find out the dependence of any dependent variable on the independent variables we consider at first the quasi-chemical reaction for the formation of La_2O_3 (Kröger–Vink notation[24]):

$$2La_{La}^{x} + 3O_{O}^{x} \Leftrightarrow 2V_{La}''' + 3V_{O}^{\cdot\cdot} + La_2O_3 \qquad (10)$$

Here La_{La}^{x} and O_{O}^{x} are regular structure elements of the perovskite, while V_{La}''' (vacancy in the La-sublattice) and $V_{O}^{\cdot\cdot}$ (vacancy in the oxygen sublattice) are irregular structure elements. The correct use of chemical potentials of structure elements has been discussed in detail in ref. 24. Eqn. (10) shows that the formation of La_2O_3 necessarily results in the formation of vacancies in both the La- and the O-sublattices. If thermodynamic equilibrium prevails we obtain from eqn. (10)

$$K_{La} = \frac{[V_{La}''']^2[V_{O}^{\cdot\cdot}]^3 a_{La_2O_3}}{[La_{La}^{x}]^2[O_{O}^{x}]^3} \qquad (11)$$

were we have assumed that the structure elements in each sublattice form an ideal solution, *i.e.* their activities are given by the corresponding site fractions which are denoted by brackets.

In addition to eqn. (10) we have the Schottky equilibrium

$$\text{nil} \Leftrightarrow V'''_{La} + V'''_{Ga} + 3V^{\bullet\bullet}_{O}, \quad K_S = [V'''_{La}][V'''_{Ga}][V^{\bullet\bullet}_{O}]^3 \qquad (12)$$

the condition of electrical neutrality

$$[Mg'_{Ga}] + 3[V'''_{La}] + 3[V'''_{Ga}] = 2[V^{\bullet\bullet}_{O}] \qquad (13)$$

the site balances in the La-, Ga- and O-sublattices

$$[La^{x}_{La}] + [V'''_{La}] = 1,\ [Ga^{x}_{Ga}] + [Mg'_{Ga}] + [V'''_{Ga}] = 1,$$
$$[O^{x}_{O}] + [V^{\bullet\bullet}_{O}] = 3 \qquad (14)$$

and the experimentally given Mg-fraction

$$\frac{[Mg'_{Ga}]}{[Ga^{x}_{Ga}]} = \frac{y}{1-y} \qquad (15)$$

Eqns. (11)–(15) form a set of seven equations from which the dependence of the seven site fractions, $[La^{x}_{La}]$, $[V'''_{La}]$, $[Ga^{x}_{Ga}]$, $[Mg'_{Ga}]$, $[V'''_{Ga}]$, $[O^{x}_{O}]$ and $[V^{\bullet\bullet}_{O}]$ on the independent thermodynamic variables can be calculated. It should be noted that in eqns. (11)–(15) the only independent thermodynamic variables are the temperature, T, the Mg-fraction, y, and the activity of La_2O_3, $a_{La_2O_3}$. There is no dependence on the oxygen activity. Only if we would consider also electronic defects, *e.g.* electrons *via* $\frac{1}{2}O_2(g) + V^{\bullet\bullet}_{O} + 2e' \Leftrightarrow O^{x}_{O}$, we would obtain an additional dependence on the oxygen activity a_{O_2}. However, from measurements of the electronic transference numbers[25] it is known that electronic defects are only minority defects and can be neglected in eqn. (13).

In Mg-doped lanthanum gallate, $LaGa_{1-y}Mg_yO_{3-y/2}$, the majority defects are Mg'_{Ga} and $V^{\bullet\bullet}_{O}$, and the condition of electrical neutrality in eqn. (13) simplifies to $[Mg'_{Ga}] = 2[V^{\bullet\bullet}_{O}]$. Thus, the oxygen vacancy fraction depends only on the Mg-fraction, $2[V^{\bullet\bullet}_{O}] = [Mg'_{Ga} \equiv y]$. In contrast, the fractions of cation vacancies, V'''_{La} and V'''_{Ga}, which are minority defects depend also on the temperature, T, and the La_2O_3-activity, $a_{La_2O_3}$(see eqns. (11) and (12)):

$$[V'''_{La}] = \sqrt{K_{La}}\left(\frac{3-y/2}{y/2}\right)^{3/2}(a_{La_2O_3})^{-1/2} \qquad (16)$$

$$[V'''_{Ga}] = \frac{K_s}{\sqrt{K_{La}}}((3-y/2)(y/2))^{-3/2}(a_{La_2O_3})^{+1/2} \qquad (17)$$

Dependent thermodynamic variables can now be calculated as a function of the independent variables. In particular, the measured chemical activities of Ga_2O_3 and MgO can be calculated considering the following quasi-chemical reactions and the corresponding equilibria:

$$2Ga^{x}_{Ga} + 3O^{x}_{O} \Leftrightarrow 2V'''_{Ga} + 3V^{\bullet\bullet}_{O} + Ga_2O_3,$$
$$K_{Ga} = \frac{[V'''_{Ga}]^2[V^{\bullet\bullet}_{O}]^3 a_{Ga_2O_3}}{[Ga^{x}_{Ga}]^2[O^{X}_{O}]^3} \qquad (18)$$

$$2Mg'_{Ga} + V^{\bullet\bullet}_{O} + Ga_2O_3 \Leftrightarrow 2Ga^{x}_{Ga} + O^{x}_{O} + 2MgO,$$
$$K_{Mg} = \frac{[Ga^{x}_{Ga}][O^{X}_{O}](a_{MgO})^2}{[Mg'_{Ga}]^2[V^{\bullet\bullet}_{O}]^3 a_{Ga_2O_3}} \qquad (19)$$

With the help of eqns. (14)–(17) the chemical activities of Ga_2O_3 and MgO can be expressed in terms of the Mg-fraction, y, and the La_2O_3-activity, $a_{La_2O_3}$.

$$a_{Ga_2O_3} = \frac{K_{La}K_{Ga}}{(K_S)^2}(1-y)^2(3-y/2)^6(a_{La_2O_3})^{-1} \qquad (20)$$

$$a_{MgO} = \sqrt{\frac{K_{La}K_{Ga}K_{Mg}}{2(K_S)^2}}y^{3/2}(3-y/2)^{5/2}(a_{La_2O_3})^{-1/2} \qquad (21)$$

The measurements of the chemical activities described in the previous sections have been performed in the two-phase region where La-rich LGM and $La_4Ga_2O_9$ coexist (see Fig. 4). Compared to the single phase region of LGM, in the two-phase region one degree of freedom is lost, which is the chemical activity of La_2O_3. Therefore, we can substitute in eqns. (16), (17), (20) and (21) $a_{La_2O_3}$ by the measured value and obtain in this way all dependent quantities at the La-rich boundary of LGM as a function of the temperature, T, and the Mg-fraction, y.

By combination of eqns. (10), (12) and (18) it can be shown easily that the combination of equilibrium constants, $K_{La}K_{Ga}/(K_S)^2$, which appears in eqns. (20) and (21), can be written as $K_{La}K_{Ga}/(K_S)^2 = (3^3 \times K_{LaGaO_3})^{-2}$, where K_{LaGaO_3} is the equilibrium constant for the formation of $LaGaO_3$ from the oxide components La_2O_3 and Ga_2O_3.

The experimental results obtained at 1800 K (see Table 6) show that the activity of La_2O_3 in the two-phase region is nearly independent of the Mg-fraction, y. Thus we can substitute $a_{La_2O_3}$ by its average value, $a^{ave}_{La_2O_3} = 0.35$,, and obtain the following expressions for the chemical activities of Ga_2O_3 and MgO in the La-rich two-phase region:

$$a_{Ga_2O_3} = \left(3^3 K_{LaGaO_3}\right)^{-2}(1-y)^2(3-y/2)^6\left(a^{ave}_{La_2O_3}\right)^{-1} \qquad (22)$$

$$a_{MgO} = \left(3^3 K_{LaGaO_3}\right)^{-2}\sqrt{\frac{K_{Mg}}{2}}y^{3/2}(3-y/2)^{5/2}\left(a^{ave}_{La_2O_3}\right)^{-1/2} \qquad (23)$$

By fitting of eqns. (22) and (23) to the experimental data (see Fig. 5) the equilibrium constants K_{LaGaO_3} and K_{Mg} at $T =$ 1800 K can determined. The results are $K_{LaGaO_3} = 30.6 \pm 2$ and $K_{Mg} = (2.4 \pm 0.6) \times 10^5$. From these values we can estimate the standard Gibbs energy for the formation of $LaGaO_3$ from the oxide components

$$\Delta_f G^0(LaGaO_3, T = 1800\ \text{K}) = -(51 \pm 1)\ \text{kJ mol}^{-1}$$

and the standard Gibbs energy for the exchange of Ga and Mg according to eqn. (19)

$$\Delta_r G^0(T = 1800\ \text{K}) = -(185 \pm 5)\ \text{kJ mol}^{-1}$$

The standard Gibbs energy for the formation of $LaGaO_3$ which was calculated from the dependence of the Ga_2O_3-activity on the Mg-fraction, y, is in good agreement with a previously published[14] value, $\Delta G^0(LaGaO_3, T = 1700\ \text{K}) = -46$ kJ mol^{-1}, which was obtained from activity measurements in the quasi-binary system La_2O_3–Ga_2O_3 ($y = 0$) at $T = 1700$ K. A comparison with reported values for the formation enthalpies,[26,27] $\Delta_f H^0 = -46.3$ kJ mol^{-1} and $\Delta_f H^0 = -51.1$ kJ mol^{-1} shows that the formation entropy of the perovskite $LaGaO_3$ is negligible.

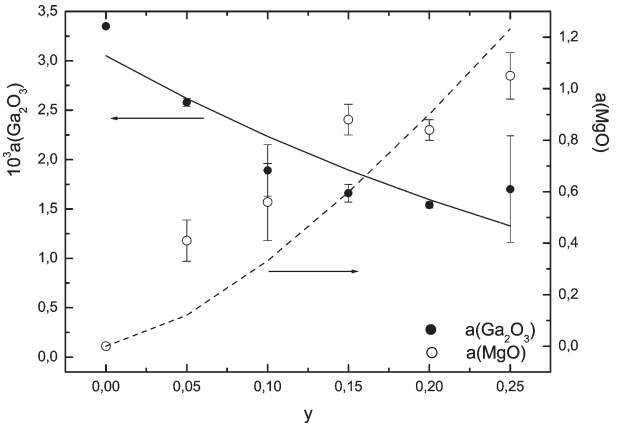

Fig. 5 Thermodynamic activities of Ga_2O_3 and MgO measured at 1800 K (symbols) and fits with eqns. (22) and (23) (lines).

The substitution of Ga by Mg described in eqn. (19) was considered in a theoretical paper[28] and the corresponding reaction enthalpy was calculated by atomistic simulations, $\Delta_r H^0 = -290$ kJ mol^{-1}. From both the measured Gibbs energy and the calculated enthalpy we can estimate the standard reaction entropy for the reaction in eqn. (19), $\Delta_r S^0 = -58$ J mol^{-1} K^{-1} It must be emphasized, however, that the fitted curve for the MgO-activity gives only a qualitative description of the measured values (see Fig. 5). The difference between the experimental data and the theoretical curve indicates deviations from ideal behavior which was assumed in our analysis and could be accounted for by considering activity coefficients.

Finally it should be emphasized that the above defect model was derived for Mg-doped lanthanum gallate, where the majority defects are Mg-ions and oxygen vacancies, $[Mg'_{Ga}] = 2[V^{\cdot\cdot}_{O}]$. This means that the model is a priori not valid for undoped lanthanum gallate, *i.e.* $y = 0$. However, the fitted activity of Ga_2O_3 in Fig. 5 describes the measured activity at $y = 0$ reasonably well, from which we can conclude that the majority disorder in pure lanthanum gallate is probably determined by unknown impurity acceptors which play the same role as the dopand Mg.

An interesting question concerns the stability field of the perovskite $LaGa_{1-y}Mg_yO_{3-y/2}$, in particular the A to B ratio or the deviation $\Delta = [La^x_{La}] - ([Ga^x_{Ga}] + [Mg'_{Ga}])$ from the exact molecularity, $\Delta = 0$. This deviation is due to different vacancy fractions in the A- and B-sublattices of the perovskite, $\Delta = [V'''_{Ga}] - [V'''_{La}]$ (see eqn. (14)). The dependence of each vacancy fraction on the activity of La_2O_3 is given by eqns. (16) and (17) and shown in a double-logarithmic plot in Fig. 6. Both vacancy fractions and the activity of La_2O_3 are normalized by their values for exact molecularity, $[V'''_{La}]^* = [V'''_{Ga}]^* = (K_S/(y/2)^3)^{1/2}$ and $a_{La_2O_3}{}^* = (K_{La}/K_S)(3-y/2)^3$, respectively. If we assume that the point of exact molecularity lies within the stability field of LGM we can estimate the maximum deviation from exact molecularity using the following arguments. From the quasi-binary system La_2O_3–Ga_2O_3 ($y = 0$) it is known[14] that the activity of La_2O_3 drops by about two orders of magnitude if we cross the stability field of $LaGaO_3$ ($a_{La_2O_3} = 0.35$ in the two-phase region $\{LaGaO_3 + La_4Ga_2O_9\}$ and $a_{La_2O_3} = 2 \times 10^{-3}$ in the two-phase region $\{LaGaO_3 + Ga_2O_3\}$). We may assume that this behavior remains qualitatively the same in Mg-doped lanthanum gallate, $LaGa_{1-y}Mg_yO_{3-y/2}$, as suggested by the phase diagram shown in Fig. 4. This means that both vacancy fractions change at maximum by one order of magnitude if we cross the stability field of LGM from the La-rich side to the Ga-rich side (see eqns. (16) and (17)). To estimate the vacancy fractions at the point of exact molecularity we need a value for the Schottky equilibrium constant, K_S. The corresponding enthalpy has been estimated from cation diffusion measurements[29] as $\Delta H_S = 1013$ kJ mol^{-1}. Neglecting the corresponding entropy we can estimate the Schottky equilibrium constant, K_S(1800 K) and the cation vacancy fractions at the point of exact molecularity. In this way we obtain at $T = 1800$ K and, *e.g.*, for $y = 0.05$ vacancy fractions $[V'''_{La}]^* = [V'''_{Ga}]^* \approx 5 \times 10^{-13}$. For pure lanthanum gallate with an assumed fraction $y = 10^{-4}$ of unknown acceptor impurities we obtain $[V'''_{La}]^* = [V'''_{Ga}]^* \approx 6 \times 10^{-9}$. Since both fractions vary at maximum by one order of magnitude when we cross the stability field of the compound, these estimates show that both pure lanthanum gallate, $LaGaO_3$ and Mg-doped lanthanum gallate, $LaGa_{1-y}Mg_yO_{3-y/2}$, exhibit extremely small cation vacancy fractions and are line compounds with very small deviations from the exact molecularity. However, it must be emphasized that this conclusion is based on the assumption that the point of exact molecularity, $\Delta = 0$, lies within the stability field of lanthanum gallate.

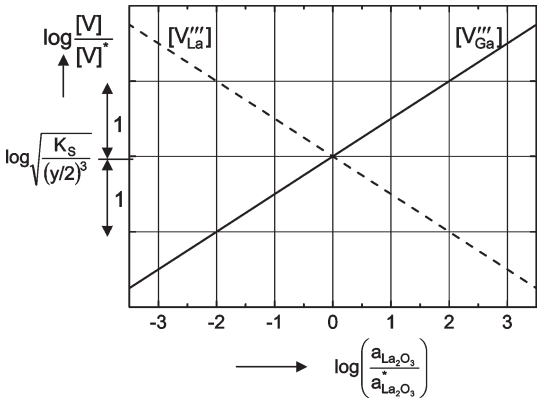

Fig. 6 Dependence of the cation vacancy fractions, V_{La} and V_{Ga}, on the activity of lanthanum oxide, $a_{La_2O_3}$, according to eqns. (16) and (17).

Conclusions

Equilibrium vaporization of the perovskite phase $LaGaO_3$ doped with different amounts of SrO and/or MgO was investigated. The thermodynamic activities of Ga_2O_3 and MgO for the La_2O_3-rich boundary of the homogeneity range of the perovskite phase $LaGa_{1-y}Mg_yO_{3-y/2}$ were determined at 1700 and 1800 K, respectively, for the concentration range $y = 0$–0.35. The thermodynamic activity of MgO showed a strong positive deviation from ideal behavior in contrast to that of Ga_2O_3 showing a negative deviation. Precise values for the thermodynamic activities of Ga_2O_3, MgO and SrO resulted also for the La_2O_3-rich boundary of the quasi-quaternary perovskites $La_{0.90}Sr_{0.10}Ga_{0.90}Mg_{0.10}O_{2.90}$, $La_{0.80}Sr_{0.20}Ga_{0.80}Mg_{0.20}O_{2.80}$ and $La_{0.90}Sr_{0.10}Ga_{0.80}Mg_{0.20}O_{2.85}$. The latter composition is discussed as electrolyte material in Solid Oxide Fuel Cells, SOFC. It is interesting to note that the thermodynamic activity of SrO and MgO showed strong positive deviation from ideal behavior as it was the case for MgO in $LaGa_{1-y}Mg_yO_{3-y/2}$.

By combining the experimental values for the activities of the oxide components with a defect chemical analysis of the quasi ternary Mg-doped lanthanum gallate, $LaGa_{1-y}Mg_yO_{3-y/2}$, it was possible (i) to model the observed dependence of the activities on the Mg-fraction, (ii) to obtain standard Gibbs energies for the formation of lanthanum gallate, $\Delta_f G^0(LaGaO_3, T = 1800\ K) = -(51 \pm 1)$ kJ mol^{-1}, and the exchange of Ga and Mg, $\Delta_r G^0(T = 1800\ K) = -(185 \pm 5)$ kJ mol^{-1}, and (iii) to show that the width of the stability field of Mg-doped lanthanum gallate is extremely small. It should be emphasized that, in principle, the combination of an experimental technique by which the oxide activities can be measured (*e.g.* KEMS) and a defect chemical analysis is necessary in all quasi-ternary (or higher) compounds where the activity of one (or more) oxide component is an independent thermodynamic variable. This is of particular importance in compounds with a very narrow stability field where the chemical composition is difficult to control.

Acknowledgements

The authors thank the Deutsche Forschungsgemeinschaft, DFG, and the International Bureau of the German Ministry of Science and Technology for financial support.

References

1 I. Ishihara, M. Honda, T. Shibayama, H. Minami, H. Nishiguchi and Y. Takita, *J. Electrochem. Soc.*, 1998, **145**, 3177.
2 T. Ishihara, H. Matsuda and Y. Takita, *J. Am. Chem. Soc.*, 1994, **116**, 3801.

3 M. Feng and J. B. Goodenough, *Eur. J. Solid State Inorg. Chem.*, 1994, **31**, 663.
4 P. Huang and A. Petric, *J. Electrochem. Soc.*, 1996, **143**, 1644.
5 K. Yamaji, T. Horita, M. Ishikawa, N. Sakai and H. Yokokawa, *Solid State Ionics*, 1998, **108**, 415.
6 K. Yamaji, T. Horita, M. Ishikawa, N. Sakai and H. Yokokawa, *Solid State Ionics*, 1999, **121**, 217.
7 K. Yamaji, T. Horita, M. Ishikawa, N. Sakai and H. Yokokawa, *Solid State Ionics*, 2000, **135**, 389.
8 W. Kuncewicz-Kupczyk, D. Kobertz, M. Miller, L. Singheiser and K. Hilpert, *J. Electrochem. Soc.*, 2001, **148**, E276.
9 A. Matraszek, D. Kobertz, L. Singheiser, K. Hilpert, W. Kuncewicz-Kupczyk and M. Miller in: *Solid Oxide Fuel Cells VII (SOFC-VII)*, ed. H. Yokokawa and S. C. Singhal Proc. vol. 2001–2016, The Electrochemical Society Proceedings Series, Pennington, NJ, 2001, pp. 319–328.
10 A. Matraszek, D. Kobertz, L. Singheiser, K. Hilpert, W. Kuncewicz-Kupczyk, M. Miller, O. Schulz and M. Martin, *Mat.-wiss. u. Werkstofftechn.*, 2002, **33**, 355.
11 O. Schulz and M. Martin, *Solid State Ionics*, 2000, **135**, 549.
12 V. L. Stolyarova and G. A. Semenov, *Mass Spectrometric Study of the Vaporization of Oxide Systems*, Wiley, New York, 1994.
13 K. Hilpert, *Rapid Commun. Mass Spectrom.*, 1991, **5**, 175.
14 W. Kuncewicz-Kupczyk, D. Kobertz, M. Miller, C. Chatillon and K. Hilpert, *J. Am. Ceram. Soc.*, 2002, **85**, 2299.
15 W. A. Chupka, M. G. Inghram and R. F. Porter, *J. Chem. Phys.*, 1956, **24**, 792.
16 R. F. Porter, W. A. Chupka and M. G. Inghram, *J. Chem. Phys.*, 1955, **23**, 1347.
17 P. J. Majewski, M. Rozumek, H. Schluckwerder and F. Aldinger, *J. Am. Ceram. Soc.*, 2001, **84**, 1093.
18 P. J. Majewski, M. Rozumek and F. Aldinger, *J. Alloys Compd.*, 2001, **329**, 253.
19 K. Huang and J. B. Goodenough, *J. Alloys Compd.*, 2000, **303–304**, 454.
20 W. Kuncewicz-Kupczyk, M. Miller and K. Hilpert, unpublished work.
21 D. H. Peck, M. Miller and K. Hilpert, *Solid State Ionics*, 2002, **147**, 29.
22 D. H. Peck, M. Miller and K. Hilpert, *Solid State Ionics*, 2001, **143**, 401.
23 D. H. Peck, M. Miller and K. Hilpert, *Solid State Ionics*, 2001, **143**, 391.
24 F. A. Kröger, *Chemistry of Imperfect Crystals*, North Holland, Amsterdam, 1964.
25 H.-J. Kim and H.-I. Yoo, *Solid State Ionics*, 2001, **140**, 105.
26 K. T. Jacob, N. Dasgupta, H. Näfe and F. Aldinger, *J. Mater. Res.*, 2000, **15**, 2836.
27 Y. Kanke and A. Navrotsky, *J. Solid State Chem.*, 1998, **141**, 424.
28 R. A. De Souza and J. Maier, *Phys. Chem. Chem. Phys.*, 2003, **5**, 740.
29 O. Schulz, M. Martin, C. Argirusis and G. Borchardt, *Phys. Chem. Chem. Phys.*, 2003, **5**, 2308.